Brazilian Dental Science

unesp
UNIVERSIDADE ESTADUAL PAULISTA
"JÚLIO DE MESQUITA FILHO"
Instituto de Ciência e Tecnologia
Campus de São José dos Campos

ORIGINAL ARTICLE

DOI: https://doi.org/10.4322/bds.2025.e4785

Does image processing improve diagnostic accuracy and differentiation between odontogenic keratocysts and simple bone cysts? A comparative study

O processamento de imagem contribui para o aumento da acurácia do diagnóstico e distinção entre queratocisto odontogênico e cisto ósseo simples? Um estudo comparative

Leticia Dantas GROSSI[1], **Kellen Cristine TJIOE**[1,2,3], **Heitor Marques HONÓRIO**[4], **Cássia Maria Fischer RUBIRA**[1], **Izabel Regina Fisher RUBIRA-BULLEN**[1]

1 – Universidade de São Paulo, Faculdade de Odontologia de Bauru, Departmento de Cirurgia, Estomatologia, Patologia e Radiologia. Bauru, SP, Brazil.
2 - Augusta University, Medical College of Georgia, Georgia Cancer Center. Augusta, GA, USA.
3 - Augusta University, Dental College of Georgia, Department of Oral Biology. Augusta, GA, USA.
4 - Universidade de São Paulo, Faculdade de Odontologia de Bauru, Departmento de Odontopediatria, Ortodontia e Saúde Coletiva. Bauru, SP, Brazil.

How to cite: Grossi LD, Tjioe KC, Honório HM, Rubira CMF, Rubira-Bullen IRF. Does image processing improve diagnostic accuracy and differentiation between odontogenic keratocysts and simple bone cysts? A comparative study. Braz Dent Sci. 2025;28(3):e4785. https://doi.org/10.4322/bds.2025.e4785

ABSTRACT

Objective: The aim of this study was to evaluate the diagnostic accuracy of image processing in differentiating odontogenic keratocysts (OKCs) and simple bone cysts (SBCs) using panoramic radiographs (OPGs) and cone-beam computed tomography (CBCT) scans. **Material and Methods:** Five images of OKCs and five of SBCs were processed using enhancement features available in GIMP software (including edge enhancement and smoothing filters) and compiled into image panels for observer analysis. A total of 20 OPG and 20 CBCT images were used—10 processed and 10 unprocessed for each modality. Eight observers with prior knowledge in Oral and Maxillofacial Radiology assessed the images in two sessions spaced two months apart. The observers were blinded to the image processing status and the imaging modality (OPG or CBCT). In the first session, six diagnostic options were provided; in the second session, the options were narrowed to two. **Results:** Multivariate analysis revealed that image processing was not a significant predictor of diagnostic accuracy ($p=0.642$ and $p=0.678$). However, both the type of lesion ($p<0.001$) and the imaging modality ($p=0.004$) significantly influenced correct diagnosis. Notably, OPG images were more likely to lead to correct answers compared to CBCT (odds ratio=3.033; 95% confidence interval=1.418–6.487; $p=0.004$). **Conclusion:** while image processing did not improve diagnostic accuracy, the imaging modality and the type of lesion had a significant impact on observer performance.

KEYWORDS

Artificial intelligence; Cone-beam computed tomography; Diagnostic imaging; Odontogenic cysts; Panoramic radiography.

RESUMO

Objetivo: O objetivo deste estudo foi avaliar a acurácia do processamento de imagem no diagnóstico e na diferenciação entre queratocisto odontogênicos (QOs) e cisto ósseo simples (COSs), utilizando radiografias panorâmicas (PANs) e tomografias computadorizadas de feixe cônico (TCFCs). **Material e Métodos:** Cinco imagens de QOs e cinco de COSs foram processadas com recursos de aprimoramento oferecidos pelo software GIMP (realce de bordas e filtros de suavização), e organizadas em painéis de imagens para análise dos avaliadores. Vinte PAN e 20 de TCFC foram utilizadas — 10 processadas e 10 não processadas para cada modalidade. Oito avaliadores com conhecimento prévio em Radiologia Oral e Maxilofacial analisaram as imagens em duas sessões,

com intervalo de dois meses entre elas. Os avaliadores desconheciam processamento das imagens e a modalidade de aquisição da imagem. Na primeira sessão, foram oferecidas seis opções diagnósticas; na segunda, o número de opções foi reduzido para duas. **Resultados:** A análise multivariada revelou que o processamento de imagem não foi um preditor significativo da acurácia diagnóstica (p=0,642 e p=0,678). No entanto, tanto o tipo de lesão (p<0,001) quanto a modalidade de imagem (p=0,004) influenciaram significativamente o acerto diagnóstico. Notavelmente, as imagens de PAN apresentaram maior chance de respostas corretas em comparação às de TCFC (OR=3,033; intervalo de confiança de 95%=1,418–6,487; p=0,004). **Conclusão:** Os resultados sugerem que, embora o processamento de imagem não tenha melhorado a acurácia diagnóstica, a modalidade de imagem e o tipo de lesão tiveram impacto significativo no desempenho dos avaliadores.

PALAVRAS-CHAVE

Inteligência artificial; Tomografia computadorizada de feixe cônico; Imagem diagnóstica; Cistos odontogênicos; Radiografia panorâmica.

INTRODUCTION

Accurate radiographic interpretation plays a critical role in the differential diagnosis of intraosseous jaw lesions. Among the most commonly used imaging modalities in Dentistry are panoramic radiography (OPG) and cone-beam computed tomography (CBCT), both offering complementary anatomical insights. OPG offers a broad, two-dimensional overview with relatively low radiation exposure, while CBCT enables high-resolution, three-dimensional visualization, which is particularly valuable for assessing complex maxillofacial structures [1].

Despite their advantages, both modalities pose diagnostic challenges, especially when evaluating lesions with overlapping radiographic features. This is particularly true for odontogenic keratocysts (OKCs) and simple bone cysts (SBCs) [2]. OKCs are typically well-defined radiolucent lesions, which may appear unilocular or multilocular, often with corticated or scalloped borders. They may cause mild buccolingual expansion, displacement of teeth, and occasionally root resorption [3]. SBCs, by contrast, usually present as unilocular radiolucencies with smooth or scalloped margins that tend to scallop between the roots of adjacent teeth. They typically lack a well-defined corticated border and rarely cause expansion or root resorption. These subtle differences can be difficult to discern, particularly on two-dimensional images, and may lead to misinterpretation. Misdiagnosis between OKCs and SBCs can lead to inappropriate clinical decisions, as their biological behaviors and treatment strategies differ significantly. OKCs are aggressive and have a higher recurrence rate, often requiring surgical enucleation or resection [3], while SBCs are generally self-limiting and may resolve spontaneously or after simple curettage [3-5].

Image processing has long been used to enhance radiographic detail by adjusting contrast, sharpening edges, and reducing noise, with the aim of improving diagnostic clarity [6]. These post-processing techniques are widely available in modern imaging software and commonly applied in clinical routines. However, although these filters may improve the visual appearance of images, they can also introduce artifacts and potentially lead to false positives or diagnostic errors [6-8]. This concern becomes even more relevant in the context of artificial intelligence (AI) applications. Deep learning algorithms, particularly convolutional neural networks (CNNs), are increasingly used to automate radiographic analysis and assist clinical decision-making [7]. These systems are highly sensitive to image structure and quality, relying on pixel-based data to recognize diagnostic patterns. Image preprocessing—such as contrast adjustment or edge enhancement—can significantly affect AI model performance, leading either to improved accuracy or to erroneous generalization [1].

OKC and SBC, although histologically distinct, often present similarly on radiographs—typically as unilocular radiolucent lesions with well-defined borders [2]. Given the recurrence risk and aggressiveness of OKCs [9] compared to the indolent and self-limiting nature of SBCs, radiographic differentiation is critical for appropriate management. Therefore, this study aimed to evaluate the impact of image processing on diagnostic accuracy and on the differentiation between odontogenic keratocysts and simple bone cysts using OPG and CBCT images. The findings are expected to contribute not only to clinical

radiology practice but also to the development of reliable AI-based diagnostic systems.

MATERIALS AND METHODS

Sample and imaging processing

This observational and analytical study was approved by the Institutional Review Board at Bauru School of Dentistry, University of São Paulo (protocol #CAAE 54911322.1.0000.5417). OKCs and SBCs were obtained from the imaging archive at the Department of Surgery, Stomatology, Pathology, and Radiology, Bauru School of Dentistry. Five OKCs and five SBCs were selected based on the following criteria: (1) imaging exams of patients with clinically and microscopically confirmed diagnosis of OKC or SBC; (2) availability of preoperative CBCT and OPG. In the absence of the preoperative OPG, panoramic reconstructions from CBCT were used; (3) high-quality images including the entire lesion and devoid of acquisition errors. The clinical features of the representative OKC and SBC can be found in Supplemental Table 1 and Supplemental File 1.

For each lesion (five OKCs and five SBCs), one OPG and one set of CBCT images from the same patient were collected. Each image set was duplicated and submitted to image processing using GNU Image Manipulation Program (GIMP) software (Figure 1). The filters applied included edge enhancement and smoothing ('Unsharp Mask' filter) using the following the parameters: Radius 7.0, Amount 0.5, Threshold 0.0. This resulted in a total of 40 images: 20 OPG (10 processed and 10 unprocessed) and 20 CBCT (10 processed and 10 unprocessed). These images were coded, sorted randomly, and inserted into slides to be distributed to the observers along with a questionnaire (Supplemental File 1).

Observers recruitment and questionnaire

Eight observers with experience in Oral and Maxillofacial Radiology (OMFR) were invited to participate in the study. They were graduate students (Master's and PhD candidates) or board-certified OMF Radiologists. All observers were required to attend two in-person sessions to respond to the questionnaire. Image evaluation was conducted individually at computers under standardized conditions for radiographic interpretation.

This study was divided into three phases (Figure 2). The phase 1 involved a questionnaire consisting of 40 randomized images, including 20 of odontogenic keratocysts and 20 of simple bone cysts. Each observer selected a diagnosis from six possible options: odontogenic keratocyst,

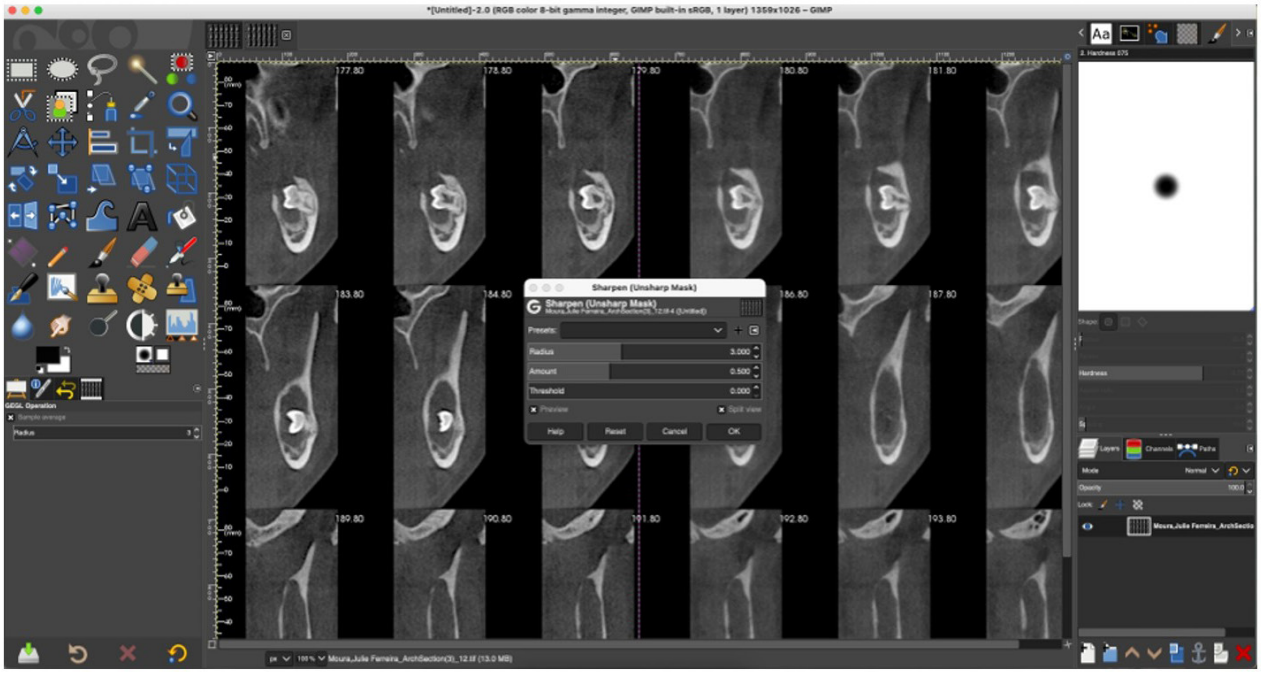

Figure 1- Screenshot of the GIMP software interface used for image processing. The figure shows an example of a radiographic image loaded into the program, with enhancement tools available through the filter menu.

dentigerous cyst, ameloblastoma, simple bone cyst, central giant cell lesion, or fibro-osseous lesion. Each image was evaluated independently, without indication of whether it had been processed or not, or whether it originated from an OPG or a CBCT scan. CBCT images included

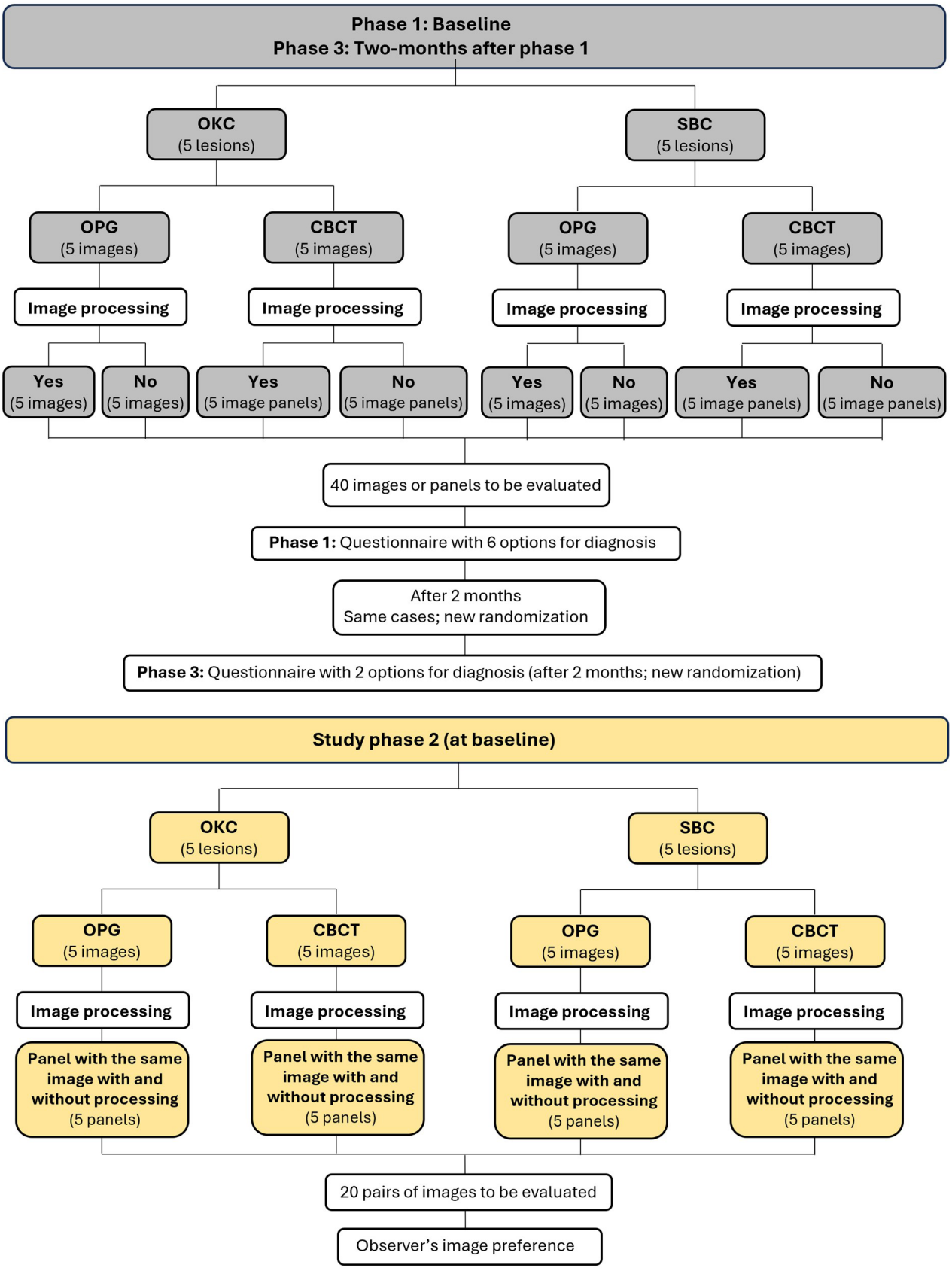

Figure 2 - Flowchart describing the study phases.

a panel of axial, coronal, and sagittal views. In addition to the primary diagnostic choice, observers were also asked whether the image clearly showed the internal content of the lesion (Yes or No), and to classify the apparent nature of the lesion content as mineralized, non-mineralized, or mixed.

In phase 2, observers were shown 20 pairs of images each consisting of a processed and an unprocessed version of the same case and were asked to choose which image they considered more appropriate for establishing a presumptive diagnosis. The images were displayed side by side, unlabeled, and in randomized order. For each image pair, the observer was instructed to select the image that they judged to offer better diagnostic value, based solely on visual clarity and diagnostic confidence. The question presented for each comparison was: "Which of these images do you consider better for making a presumptive diagnosis?". Observers were unaware of which image had been processed and were required to make a selection based exclusively on their diagnostic perception.

After a two-month interval, the phase 3 was conducted with the same observers and using the same images in a different randomized order. This time, diagnostic options were limited to two: OKC and SBC. For each image, observers answered three questions. First, they were asked to indicate their presumptive diagnosis by selecting either OKC or SBC. Second, they were asked whether the lesion's internal content was clearly visible, responding with either "yes" or "no." Third, they classified the apparent content of the lesion as mineralized, non-mineralized, or mixed. This simplified evaluation aimed to reduce diagnostic ambiguity and assess whether lesion perception and image characteristics influenced diagnostic accuracy.

Sample size and power analysis

A formal power analysis was conducted using G*Power, considering a binary outcome (correct vs. incorrect diagnosis) in a repeated-measures design. Assuming a medium effect size (Cohen's $w = 0.3$), a power of 80% ($1 - \beta = 0.80$), and an alpha level of 0.05, the minimum required sample size was calculated to be 88 observations per group. In our study, each of the 8 observers assessed 40 images (20 OPG and 20 CBCT), totaling 320 observations per session and 640 across both sessions. This repeated assessment structure significantly increased the power of the study, compensating for the relatively small number of unique image cases.

Although only 10 unique cases (5 OKCs and 5 SBCs) were used per modality, the multiple assessments by blinded and independent observers, spaced two months apart, provided sufficient data points to detect statistically significant effects related to lesion type and imaging modality. This design is consistent with diagnostic accuracy studies in oral radiology literature that utilize observer-based performance rather than large case numbers.

Data analysis

All statistical analyses were performed using SPSS version 28.0.1.1. Descriptive statistics were used to summarize observer responses and diagnostic accuracy across groups. Diagnostic accuracy (correct vs. incorrect diagnosis) was the binary outcome variable. Inter-examiner agreement was evaluated using Fleiss' kappa, considering the multiple raters assessing the same set of cases. Kappa values were interpreted based on standard thresholds: slight (0–0.20), fair (0.21–0.40), moderate (0.41–0.60), substantial (0.61–0.80), and almost perfect (>0.80). Associations between diagnostic accuracy and explanatory variables (image processing, imaging modality, lesion type) were assessed using multivariate logistic regression models. Significance was set at $p < 0.05$ for all tests.

RESULTS

In Phase 1, which involved selecting one diagnosis among six possible options, a total of 320 responses were recorded, corresponding to 40 images evaluated by 8 observers. Inter-examiner agreement was moderate overall (Fleiss' kappa = 0.459). These findings suggest a reasonable level of diagnostic reproducibility, though observer variability remained. Of the 160 responses related to OKCs, only 41 were correct, resulting in a diagnostic accuracy of 25.6% (Table I). The majority of incorrect responses for OKCs were misclassified as dentigerous cysts (35.5%) or ameloblastomas (30.6%). For SBCs, also represented by 160 responses, 72 were correct, yielding an accuracy rate of 45%. Altogether, the overall diagnostic accuracy in

this phase was 35.31% (113 correct responses out of 320).

When comparing diagnostic performance by imaging modality, OPG yielded more accurate results than CBCT. Specifically, 32 correct responses were obtained from unprocessed OPG images (Table II) and 32 from processed OPG images, while CBCT images yielded 23 and 26 correct responses in unprocessed and processed formats, respectively. These findings demonstrate that OPG images produced higher diagnostic accuracy than CBCT, and that image processing did not significantly influence diagnostic performance.

In Phase 2, a total of 20 image pairs, each composed of a processed and an unprocessed version of the same case—were presented to the observers, resulting in 160 responses. For each pair, observers were asked to choose the image they considered more appropriate for making a presumptive diagnosis. Among the 160 responses, 113 selections (71%) favored the processed images, while 47 selections (29%) favored the unprocessed ones (Figure 3). This indicates a clear visual preference for processed images, although this preference did not correspond to improved diagnostic accuracy, as seen in Phase 1.

In Phase 3, conducted two months after the initial evaluations, the same 40 images were re-evaluated by the same group of eight observers in a newly randomized order. This time, only two diagnostic options were provided: OKC and SBC. A total of 320 responses were recorded (Table I). For OKC cases, 147 out of 160 responses were

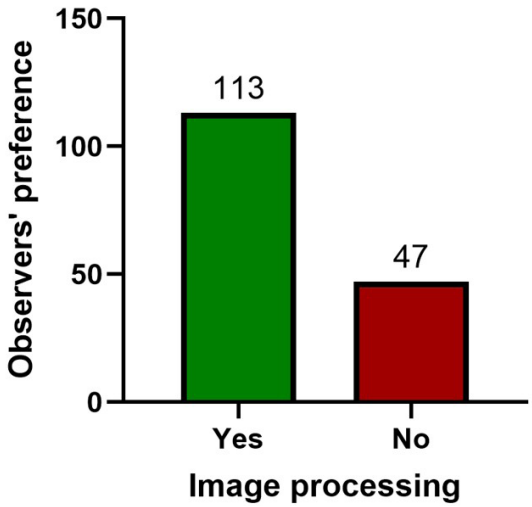

Figure 3 - Distribution of observer responses based on image preference. Each of the 20 image pairs consisted of identical images presented in both processed and unprocessed formats, with the order randomized. Eight observers were instructed to indicate the image they preferred for diagnostic interpretation.

Table I – Distribution of responses from the first and third study phases according to the correct diagnosis

Study phase	Correct Diagnosis	Responses							
		OKC n (%)	SBC n (%)	AMB n (%)	CGCL n (%)	DC n (%)	FO n (%)	Total n (%)	Correct n (%)
1[a]	OKC	41 (25.6)	1 (0.6)	49 (30.6)	11 (6.9)	57 (35.5)	1 (0.6)	160 (100.0)	41 (25.6)
	SBC	24 (15.0)	72 (45.0)	14 (8.8)	13 (8.1)	10 (6.3)	27 (16.8)	160 (100.0)	72 (45.0)
3[a]	OKC	147 (91.9)	13 (8.1)	-	-	-	-	160 (100.0)	147 (91.9)
	SBC	41 (25.6)	119 (74.4)	-	-	-	-	160 (100.0)	119 (74.4)

AMB: Ameloblastoma, DC: Dentigerous cyst, CGCL: Central Giant Cell Lesion, FO: Fibrous-osseous lesion; OKC: Odontogenic keratocyst; SBC: Simple bone cyst. [a]Phase 1: Six options for diagnosis / Phase 3: Two options for diagnosis.

Table II – Distribution of the correct answers by image acquisition method and presence or absence of image processing.

Image Acquisition Method	Image Processing	Phase 1[a] Correct responses n (%)	Phase 3[a] Correct responses n (%)
OPG	No	32 (28.3)	70 (26.3)
	Yes	32 (28.3)	70 (26.3)
CBCT	No	23 (20.4)	63 (23.7)
	Yes	26 (23.0)	63 (23.7)
Total		113[b] (100)	266[c] (100)

OPG: Panoramic radiography; CBCT: Cone beam computed tomography. [a]Phase 1: Six options for diagnosis / Phase 3: Two options for diagnosis. [b]Correct responses: 113 out of 320. [c]Correct responses: 266 out of 320.

correct, yielding a diagnostic accuracy of 91.9%, with only 13 cases misclassified as SBC. For SBCs, 119 out of 160 responses were correct (74.4%), while 41 were misidentified as OKCs (Table I). These results indicate a substantial improvement in diagnostic accuracy compared to Phase 1, especially for OKCs, due to the reduced number of diagnostic options.

Across both diagnostic phases (phases 1 and 3), observers were also asked to evaluate image clarity and the apparent nature of lesion content. In Phase 1, 91 of the 113 correct responses (80.5%) were associated with images labeled as "lesion clearly visible", while 163 of the 207 incorrect responses (78.8%) were also labeled as "lesion clearly visible" (Table III). In Phase 3, 174 of the 266 correct responses (65.5%) were rated as clear, and 29 of the 54 incorrect responses (53.7%) were similarly labeled. These results suggest that perceived image clarity did not significantly correlate with diagnostic success in either evaluation. Imaging processing did not impact observers' perception on the clarity of the lesion image (Supplemental Table 2).

Lesion content was most frequently described as "non-mineralized" in correct responses. In Phase 1, 101 out of 113 correct answers (89.3%) were associated with non-mineralized interpretations (Supplemental Table 3), and in Phase 3, 224 of the 265 valid correct responses (84.5%) were also interpreted as non-mineralized. This pattern indicates a consistent association between perceived non-mineralized content and diagnostic accuracy across both diagnostic tasks.

Finally, a multivariate logistic regression analysis was conducted to identify predictors of diagnostic performance. In Phase 1, lesion type was statistically significant, with the odds of correctly diagnosing a OKC 2.48 times higher (Table IV) than for an SBC. However, in Phase 3, SBC were more accurately diagnosed than OKC (OR: 0.281; 95% CI: 0.141-0.561; $p<0.001$). Image clarity was not significantly associated with diagnostic accuracy in either phase ($p = 0.402$ and $p = 0.136$), nor was image processing ($p = 0.642$ and $p = 0.678$). However, imaging modality showed a significant effect in Phase 3 ($p = 0.004$), with OPG yielding higher diagnostic accuracy than CBCT.

DISCUSSION

Numerous digital tools have been developed to improve diagnostic accuracy, including commonly used image filters designed to enhance visualization and aid diagnosis. However, there are still relatively few studies evaluating the true effectiveness of these filters [10-12]. The filters applied in this study were intended to remove undesirable image characteristics. High-pass and low-pass filters modify signals above or below a selected frequency. High-pass filters sharpen the image and are therefore also referred to as edge-enhancing or sharpening filters [13]. These filters accentuate the borders between regions of differing intensities, enhancing the contrast between adjacent pixels and gray levels; however, they also increase image noise [14]. In contrast, low-pass filters reduce high-frequency noise by smoothing and homogenizing pixel values and image boundaries [13].

The diagnostic differences observed between OKCs and SBCs across imaging modalities can be partially explained by their fine radiological characteristics [3]. OKCs typically present as well-defined, unilocular or multilocular radiolucencies with corticated borders and, in some cases, scalloped margins [3]. They may expand the cortical plates but tend to do so with minimal bone destruction. On OPG, these features often remain distinct due to the global view and high contrast between the lesion and surrounding

Table III – Distribution of the responses according to the observers' impression on the image clarity and their relationship with correct answers.

	Phase 1[a] responses		Phase 3[a] responses	
Lesion clearly visible[b]	Correct	Incorrect	Correct	Incorrect
	n (%)	n (%)	n (%)	n (%)
Yes	91 (80.5)	163 (78.8)	174 (65.5)	29 (53.7)
No	22 (19.5)	44 (21.2)	92 (34.5)	25 (46.3)
Total	113 (100.0)	207 (100.0)	266 (100.0)	54 (100.0)

[a]Phase 1: Six options for diagnosis / Phase 3: Two options for diagnosis. [b]Considered the image to provide a clear view of the lesion.

Table IV – Predictive model for the correct diagnosis.

Predictor	Phase 1[a] responses		Phase 3[a] responses	
	ORb (95% CI)	p	OR[b] (95% CI)	p
Lesion		<0.001*		<0.001*
SBC	Reference		Reference	
OKC	2.488 (1.523-4.040)		0.281 (0.141-0.561)	
Image acquisition method				0.004*
CBCT	Reference	0.052	Reference	
OPG	1.634 (0.996-2.680)		3.033 (1.418-6.487)	
Imaging processing		0.642		0.678
Yes	Reference		Reference	
No	1.120 (0.694 1.805)		0.875 (0.467 1.642)	
Lesion clearly visible		0.402		0.136
No	Reference		Reference	
Yes	1.311 (0.695 2.470)		1.810 (0.830-3.949)	
Lesion content				
Mineralized	Reference		Reference	
Non-mineralized	1.598 (0.721-3.587)	0.255	2.809 (1.368-5.768)	0.005*
Mixed	1.653 (0.198-13.792)	0.643	-	-

OR: Odds Ratio; CI: Confidence interval. [a]Phase 1: Six options for diagnosis / Phase 3: Two options for diagnosis. [b]Binomial multivariate logistic regression.*Statistically significant.

bone. SBCs, by contrast, usually appear as unilocular radiolucencies with ill-defined or scalloped borders that may closely follow the contour of adjacent roots [5]. They often lack a corticated margin and do not cause root resorption or significant expansion. On CBCT, the detailed cross-sectional views can paradoxically reduce interpretive clarity in SBCs, especially when the lesion borders blend with trabecular bone or are superimposed by artifacts [5].

OKCs and SBCs share certain radiographic characteristics with other lesions, which can lead to misdiagnosis. In Phase 1, when six diagnostic options were available, OKCs were frequently misclassified as dentigerous cysts or ameloblastomas before being correctly identified as OKC. This misclassification is likely due to the overlapping radiographic features such as unilocular or multilocular with scalloped borders in ameloblastomas [15]. Interestingly, when six diagnostic options were presented, some observers diagnosed SBCs as fibro-osseous lesions. However, most classified the content of these lesions as non-mineralized, regardless of imaging modality or filter application, which contradicts the typical appearance of fibro-osseous lesions, as they usually present mineralized internal content. Another key finding was that reducing diagnostic complexity by offering only two diagnostic choices (Phase 3) significantly increased diagnostic accuracy for both OKC and SBC. When comparing diagnostic accuracy by imaging modality, panoramic radiographs produced a higher percentage of correct responses than CBCT in both questionnaires. Although the difference was not statistically significant in Phase 1 (six-option format), OPG was associated with higher odds of correct diagnosis than CBCT (OR= 1.634; 95% CI= 0.996–2.680; p= 0.052). However, in Phase 3, after controlling for confounding factors, the imaging modality became a statistically significant predictor of diagnostic accuracy (OR= 3.033; CI= 1.418–6.487; p= 0.004). This may be due to observers being more familiar with OPG interpretation compared to CBCT, a trend common among general dental practitioners [16].

In terms of image clarity perception, observers consistently reported better visibility of lesion content when viewing CBCT images. However, in both study phases, a slightly higher percentage of participants favored the processed images, regardless of modality. This higher diagnostic accuracy of OPG over CBCT in this study may reflect the clearer visualization of overall lesion shape, location, and cortical relationship in a single plane. Conversely, CBCT,

while offering fine spatial detail, may introduce complexity through multiple slices, potentially diluting key visual cues in non-expansile lesions like SBCs. Image processing, though visually preferred by observers, did not significantly improve diagnostic accuracy — possibly because it emphasized edge contrast without meaningfully enhancing the radiographic hallmarks needed to differentiate between the two entities. Despite this trend, the difference was not statistically significant.

Regarding lesion content, the majority of responses classified the lesions as non-mineralized in both study phases. Both OPG and CBCT images that had been processed were more frequently associated with this classification, possibly due to the smoothing effect of the applied filters.

When the number of correct responses was compared with observers' judgment regarding clarity of lesion content, a higher percentage of correct responses was associated with images labeled "clear." However, this was also true for a majority of incorrect responses, indicating that perceived clarity alone did not predict diagnostic accuracy. Processed images were generally preferred over unprocessed ones. Even though image processing did not impact diagnostic accuracy, this suggests that post-processing operations influence image appeal without necessarily improving clinical decision-making[11]. Recent studies have shown that some enhancement filters can alter image sharpness and contrast in ways that introduce artifacts, potentially impairing diagnostic accuracy [11, 17, 18].

A recent study evaluating the impact of digital filters on the diagnosis of root resorption using enhancement filters from the VistaScan and Digora Toto systems found no scientific evidence that these filters affect diagnostic performance for internal or external root resorption[10-12].

Although this study demonstrates that image processing filters did not significantly impact diagnostic accuracy for OKCs and SBCs, the preference shown by observers for processed images highlights a potential avenue for clinical enhancement—especially when combined with artificial intelligence (AI) tools. Recent advances in deep learning models applied to dental radiography have enabled automatic classification and detection of pathological features, improving both speed and diagnostic accuracy [7, 19].

For instance, Sim et al. [19] developed a deep learning model based solely on panoramic radiographs to differentiate between OKC and SBC, achieving an overall accuracy of 0.829 [19]. This supports the notion that even subtle radiographic distinctions between these lesions can be identified by AI models when properly trained. Similarly, Katsumata (2023) discussed the utility of deep learning tasks—such as classification, segmentation, and detection—in enhancing dental image interpretation, including automatic identification of maxillofacial lesions and generation of diagnostic reports using natural language processing [7].

Such AI capabilities could be strengthened by optimized image preprocessing techniques, including filtering and segmentation. While our study did not find significant diagnostic gains with manual image filtering, standardized preprocessing may still play a foundational role in AI workflows by improving data quality and reducing noise, as highlighted in recent AI model training protocols [7, 19].

CONCLUSION

Although the current results suggest limited standalone value of image enhancement filters for human diagnostic accuracy, their integration into AI-powered diagnostic systems could offer synergistic benefits, streamlining workflows and aiding clinicians in complex differential diagnoses. Given that artificial intelligence systems rely on large volumes of well-annotated and high-quality imaging data for training, ensuring consistency and clarity in image presentation—even without diagnostic gain—may enhance the efficiency of data annotation and classification. Thus, understanding the effects of image preprocessing remains crucial in the context of developing robust AI-assisted diagnostic tools.

Acknowledgements

None to declare.

Author's Contributions

KCT, IRFRB: Conceptualization. LDG: Data Curation. HMH, CMFR: Formal Analysis. IRFRB: Funding Acquisition. LDG: Investigation. KCT, HMH, CMFR, IRFRB: Methodology. LDG: Project Administration. KCT, IRFRB: Supervision. LDG:

Writing – Original Draft Preparation. KCT, HMH, CMFR, IRFRB: Writing – Review & Editing.

Conflict of interest

None to declare.

Funding

This study was supported by the Coordination for the Improvement of Higher Education Personnel – Brazil (CAPES) – Finance Code 001.

Regulatory Statement

This study was approved by the Institutional Review Board at Bauru School of Dentistry, University of São Paulo (protocol #CAAE 54911322.1.0000.5417).

REFERENCES

1. Kwon T, Choi DI, Hwang J, Lee T, Lee I, Cho S. Panoramic dental tomosynthesis imaging by use of CBCT projection data. Sci Rep. 2023;13(1):8817. http://doi.org/10.1038/s41598-023-35805-1. PMid:37258603.
2. Theodorou SJ, Theodorou DJ, Sartoris DJ. Imaging characteristics of neoplasms and other lesions of the jawbones: part 2. Odontogenic tumor-mimickers and tumor-like lesions. Clin Imaging. 2007;31(2):120-6. http://doi.org/10.1016/j.clinimag.2006.12.021. PMid:17320779.
3. Stoelinga PJW. The odontogenic keratocyst revisited. Int J Oral Maxillofac Implants. 2022;51(11):1420-3. http://doi.org/10.1016/j.ijom.2022.02.005. PMid:35277291.
4. Lima LB, Freitas SA Fo, Paulo LFB, Servato JP, Rosa RR, Faria PR, et al. Simple bone cyst: description of 60 cases seen at a Brazilian School of Dentistry and review of international literature. Med Oral Patol Oral Cir Bucal. 2020;25(5):e616-25. http://doi.org/10.4317/medoral.23638. PMid:32683391.
5. Suei Y, Taguchi A, Tanimoto K. Simple bone cyst of the jaws: evaluation of treatment outcome by review of 132 cases. J Oral Maxillofac Surg. 2007;65(5):918-23. http://doi.org/10.1016/j.joms.2006.06.297. PMid:17448841.
6. Roman JCM, Fretes VR, Adorno CG, Silva RG, Noguera JLV, Legal-Ayala H, et al. Panoramic dental radiography image enhancement using multiscale mathematical morphology. Sensors. 2021;21(9):3110. http://doi.org/10.3390/s21093110. PMid:33946991.
7. Katsumata A. Deep learning and artificial intelligence in dental diagnostic imaging. Jpn Dent Sci Rev. 2023;59:329-33. http://doi.org/10.1016/j.jdsr.2023.09.004. PMid:37811196.
8. Oliveira V, Roseira V, Santos L, Rovai E, Marco A, Jardini M, et al. Utilizing Texture Analysis technique in diagnostic imaging at Dentistry: innovations and applications. Braz Dent Sci. 2024;27(4):1-9. http://doi.org/10.4322/bds.2024.e4342.
9. Henriques J, Silva K, Paula C, Lima L, Paulo L, Faria P. Recurrent odontogenic keratocyst and the use of Carnoy's solution: a case report. Braz Dent Sci. 2024;27(3):1-9. http://doi.org/10.4322/bds.2024.e4337.
10. Brasil DM, Yamasaki MC, Santaella GM, Guido MCZ, Freitas DQ, Haiter-Neto F. Correction to influence of VistaScan image enhancement filters on diagnosis of simulated periapical lesions on intraoral radiographs. Dentomaxillofac Radiol. 2019;48(8):20180146c. http://doi.org/10.1259/dmfr.20180146. PMid:31592696.
11. Oliveira-Santos N, Gaeta-Araujo H, Ruiz DC, Nascimento EHL, Cral WG, Oliveira-Santos C, et al. The impact of digital filters on the diagnosis of simulated root resorptions in digital radiographic systems. Clin Oral Investig. 2022;26(7):4743-52. http://doi.org/10.1007/s00784-022-04438-5. PMid:35267096.
12. Wanderley VA, Oliveira ML, Silva ALP, Tosoni GM. Evaluation of the combined assessment of two digital enhancement filters in periapical radiographs obtained with different projection angles in the detection of simulated dental root fractures. Oral Radiol. 2022;38(2):234-9. http://doi.org/10.1007/s11282-021-00550-6. PMid:34195932.
13. Lehmann TM, Troeltsch E, Spitzer K. Image processing and enhancement provided by commercial dental software programs. Dentomaxillofac Radiol. 2002;31(4):264-72. http://doi.org/10.1038/sj.dmfr.4600707. PMid:12087444.
14. Brettle D, Carmichael F. The impact of digital image processing artefacts mimicking pathological features associated with restorations. Br Dent J. 2011;211(4):167-70. http://doi.org/10.1038/sj.bdj.2011.676. PMid:21869791.
15. Liu Z, Liu J, Zhou Z, Zhang Q, Wu H, Zhai G, et al. Differential diagnosis of ameloblastoma and odontogenic keratocyst by machine learning of panoramic radiographs. Int J Comput Assist Radiol Surg. 2021;16(3):415-22. http://doi.org/10.1007/s11548-021-02309-0. PMid:33547985.
16. Salemi F, Shokri A, Foroozandeh M, Farhadian M, Yeganeh A. Knowledge level of Iranian dental practitioners towards digital radiography and cone-beam computed tomography. Braz Dent Sci. 2021;24(2):1-10. http://doi.org/10.14295/bds.2021.v24i2.2442.
17. Brasil DM, Yamasaki MC, Santaella GM, Guido MCZ, Freitas DQ, Haiter-Neto F. Influence of VistaScan image enhancement filters on diagnosis of simulated periapical lesions on intraoral radiographs. Dentomaxillofac Radiol. 2019;48(2):20180146. http://doi.org/10.1259/dmfr.20180146. PMid:30260235.
18. Clark JL, Wadhwani CP, Abramovitch K, Rice DD, Kattadiyil MT. Effect of image sharpening on radiographic image quality. J Prosthet Dent. 2018;120(6):927-33. http://doi.org/10.1016/j.prosdent.2018.03.034. PMid:30166247.
19. Sim SY, Hwang J, Ryu J, Kim H, Kim EJ, Lee JY. Differential diagnosis of OKC and SBC on panoramic radiographs: leveraging deep learning algorithms. Diagnostics. 2024;14(11):1144. http://doi.org/10.3390/diagnostics14111144. PMid:38893670.

Kellen Cristine Tjioe
(Corresponding address)
Georgia Cancer Center, Augusta University, 1410 Laney Walker Blv, CN2236B, Augusta GA 30912, USA.
Email: ktjioe@augusta.edu

Editor: Daniel Cohen Goldemberg

Date submitted: 2025 Apr 24
Accept submission: 2025 Jul 03

Supplementary Material

Supplementary material accompanies this paper.

Supplemental File 1. Study phases 1 and 3

This material is available as part of the online article at

https://ojs.ict.unesp.br/index.php/cob/article/view/4785/5049

Appendix 1. Supplemental Tables

Supplemental Table 1 – Clinical features of the lesions included in the present study

N	Diagnosis	Gender	Age at diagnosis	Location	Tooth involvement
1	Odontogenic keratocyst	Male	17	Right, posterior mandible	Yes
2		Male	32	Left, posterior mandible	Yes
3		Female	16	Left, posterior mandible	Yes
4		Female	23	Anterior mandible	No
5		Male	42	Right, posterior mandible	No
6	Simple bone cyst	Male	14	Anterior mandible	No
7		Male	15	Right, mandible	No
8		Male	21	Right, posterior mandible	No
9		Female	11	Right, mandible	No
10		Male	22	Right, mandible	No

Supplemental Table 2 – Responses regarding lesion clarity based on image acquisition method and presence or absence of image processing

Image Acquisition Method	Image Processing	Phase 1[a] Lesion clearly visible n (%)	Phase 3[a] Lesion clearly visible n (%)
OPG	No	55 (68.7)	38 (47.5)
	Yes	54 (67.5)	32 (40.0)
CBCT	No	70 (87.5)	70 (87.5)
	Yes	75 (93.7)	63 (78.7)
Total		254[b] (100)	203[c] (100)

OPG: Panoramic radiography CBCT: Cone beam computed tomography. [a]Phase 1: Six options for diagnosis / Phase 3: Two options for diagnosis. [b]Responses considering the image to provide a clear view of the lesion: 254 out of 320. [c]Responses considering the image to provide a clear view of the lesion: 203 out of 320.

Supplemental Table 3 – Distribution of the responses according to observers' perception on lesion content

Perception of lesion content	Phase 1[a] responses		Phase 3[a] responses	
	Correct n (%)	Incorrect n (%)	Correct n (%)	Incorrect n (%)
Mineralized	10 (8.8)	26 (12.6)	41 (15.5)	20 (37.0)
Non-mineralized	101 (89.3)	178 (86.4)	224 (84.5)	34 (63.0)
Mixed	2 (1.9)	2 (1.0)	0 (0.0)	0 (0.0)
Total	113 (100.0)	206 (100.0)	265 (100.0)	54 (100.0)

[a]Phase 1: Six options for diagnosis / Phase 3: Two options for diagnosis. [b]Binomial multivariate logistic regression.